Electron Paramagnetic Spectroscopy Study on Nanodiamonds

Sarah Garifo[1], **Dimitri Stanicki**[1], **Philippe Mellet**[3], **Rémi Abergel**[4], **Sylvain Durand**[4], **Robert N. Muller**[1,2], **Yves-Michel Frapart**[5], **Sophie Laurent**[1,2]

[1] General, Organic and Biomedical Chemistry Unit, NMR and Molecular Imaging Laboratory, University of Mons (UMONS), 7000 Mons, BELGIUM
[2] Center for Microscopy and Molecular Imaging (CMMI), 6041 Gosselies, BELGIUM
[3] Centre de Résonance Magnétique des Systèmes Biologiques UMR 5536, CNRS, Université de Bordeaux, 33076 Bordeaux Cedex, FRANCE
[4] Mathématiques Appliquées à Paris 5 (MAP5), UMR 8145, CNRS, Université de Paris Cité, 75270 Paris, FRANCE
[5] Laboratoire de Chimie Biochimie Pharmacologiques et Toxicologiques (LCBPT), UMR 8601, CNRS, Université de Paris Cité, 75270 Paris, FRANCE

I. Context

Recent advances in nanotechnology have attracted considerable interest for nanodiamonds (NDs) thanks to their remarkable intrinsic properties (*e.g.*, chemical stability, magnetic and optical properties). The relative stability of radical-like centers entrapped inside NDs constitutes a main interest for versatile applications such as EPR imaging.

Here, we describe the development and design of a nanodiamond strategy (*e.g.*, particle origin, surface oxidation, size exclusion) to demonstrate high EPR spectroscopic and imaging feasibilities. To achieve this, mathematical and IT procedures were developed and allowed experimental evidence of the conditions required for optimal phantom images resolution.

The ability to perform low frequency EPR resolution imaging in combination with the stable intrinsic properties of NDs, raises the possibility of performing non-invasive tracking for biological purposes.

II. Objectives

- I
  - Study of two types of NDs as platform
  - Evaluation of intrinsic EPR properties
  - Physicochemical treatments to decrease the broad EPR contribution
- II
  - L-Band EPR imaging optimizations
  - Phantoms imaging feasibility studies
- III
  - Surface grafting procedure
  - *In vitro* evaluation
  - Further use as an EPR imaging platform for biomedical applications

Commercial nanodiamond particles (size smaller than 100 nm)

- Of dynamic synthesis — *Explosives, under O_2 deficient atmosphere* → Explosives precursor → **DET NDs**
- Of static synthesis — *High-pressure high-temperature* → Grinding of µ-sized HPHT diamond → **HPHT NDs**

III. Methodology and Results

I. Experimental setup and physicochemical characterizations

General scheme of a ND as an unpaired e⁻ carrier

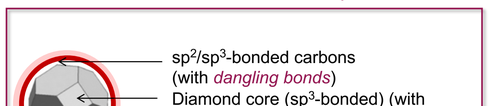

DET-asrec

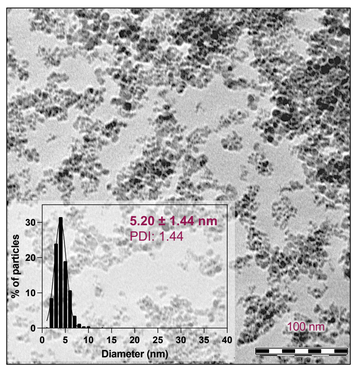

HPHT-18

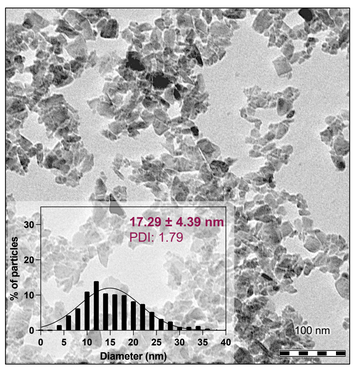

Size exclusion
16,800 g
60 min-increments
HPHT-sub18nm fractions

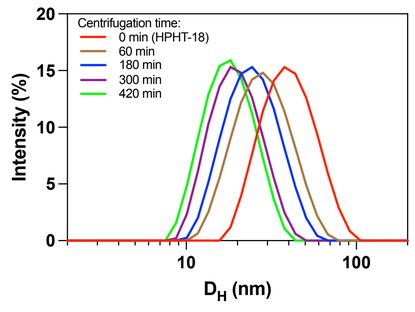

- Broader HPHT size distribution due to the grinding process → size exclusion

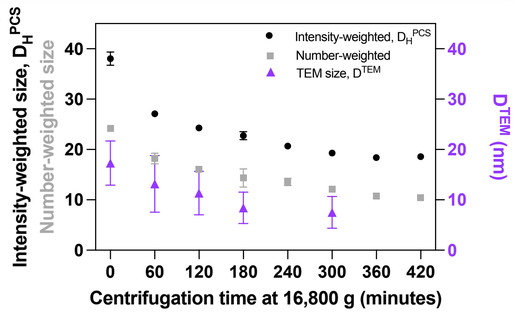

- Particles size closed to the one of DET were isolated from HPHT-18 sample

- Thermal oxidation of the ND powders in a muffle furnace
- Dispersion in H_2O using an ultrasound probe sonicator (200 W, 24 kHz)

Oxidation by air-annealing

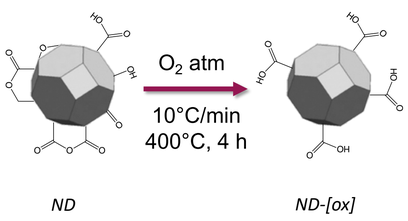

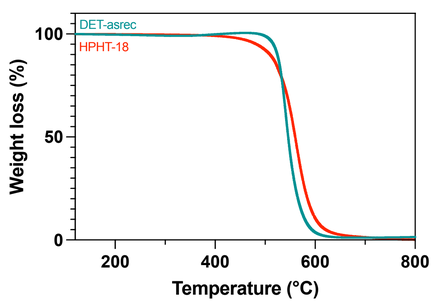

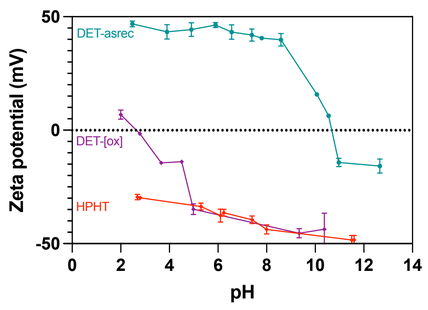

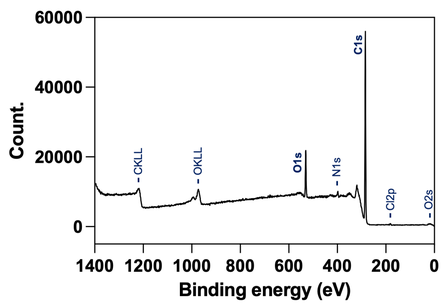

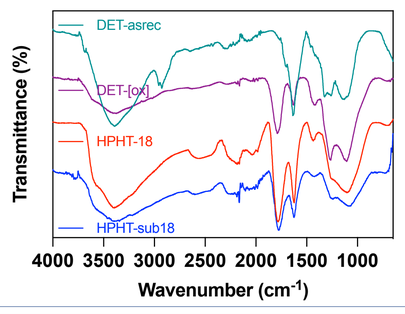

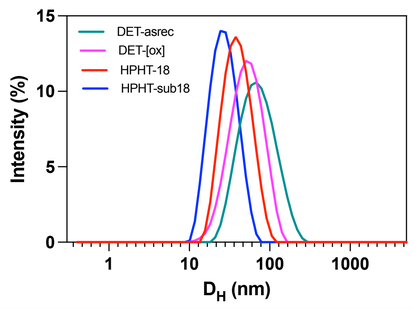

XPS data

System	C1s (%)	O1s (%)	Ratio O/C
DET-asrec	94.2	3.8	0.04
DET-[ox]	89.2	9.4	0.10

- Controlled annealing in air leads to efficient purification of the carbon ND shells
- Structural and chemical correlations confirm surface modification for DET while no significant differences were observed for HPHT
- Surface carboxylic acid functions
- HPHT size below 10 nm may facilitate easier cell penetration for (*in vitro*) medical imaging and to decrease EPR linewidth

II. EPR spectroscopy and phantom imaging study

- *X-band EPR spectra*

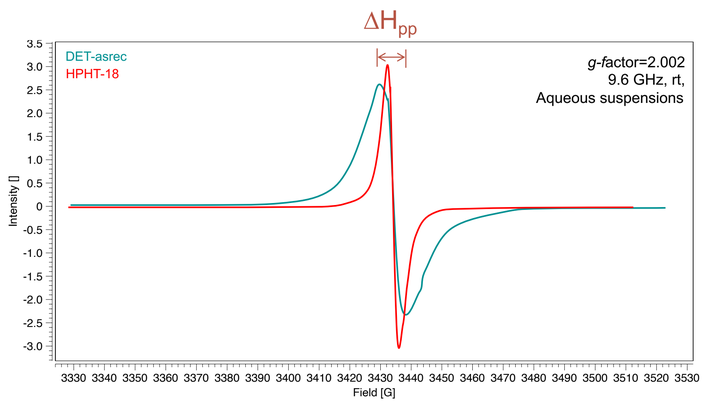

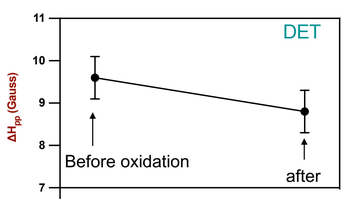

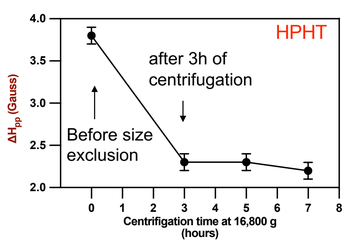

Electron spin resonance spectroscopy was performed to evaluate the influence of the treatments. Their experimental EPR spectrum can be assumed as a sum of two components of single lines with the same *g*-factor (*g* = 2.0028) but having different linewidth contributions: a **broad spin-1/2** Lorentzian component assigned to carbon dangling bonds on the particle surface and a **narrow spin-1/2** Lorentzian component attributed to defects within the diamond lattice. The observed EPR line shapes were characterized with peak-to-peak resonance width (ΔH_{pp}) according to some parameters (*e.g.*, NDs origin, treatments). Since the resolution in EPR imaging is closely proportional to:

$$\text{Resolution} \propto \Delta H_{pp}/\nabla$$

Thus, linewidth values were studied and modified by applying surface modification and size exclusion to reduce the broad component of the signal (TEMPO, ΔH_{pp}=1.4 G).

L-band EPR phantom imaging experiments (1 GHz) were evaluated and optimized using:

- Adequate mathematical procedures
- PTFE capillaries with different Ø (X-scanner)

Summary of the physicochemical properties of the nanodiamonds

Parameter / System (10 mg mL⁻¹)	Surface: ζ (pH=7.3±0.1) (mV)	Size: D_H^{PCS} (nm)	Size: D^{TEM} (nm)	Size: PDI	EPR data: ΔH_{pp} (Gauss)	EPR data: *R* (mm)	EPR data: N_S (spin/g)	NMR: ^1H R_1 20 MHz, 37°C (s^{-1})
DET-asrec	41.9 ± 2.7	62.9 ± 0.7	5.2 ± 1.4	1.4	9.6	>2	6.6 10^{19}	0.69
DET-[ox]	-39.9 ± 2.2	45.6 ± 0.4	4.5 ± 1.2	1.4	8.8	>2	5.8 10^{19}	0.62
HPHT-18	-39.5 ± 1.7	36.1 ± 0.2	17.3 ± 4.4	1.8	3.8	<1	1.5 10^{19}	0.49
HPHT-sub3h	-36.4 ± 1.5	23.9 ± 0.3	8.4 ± 3.1	1.5	2.3	0.5	1.3 10^{19}	0.36
HPHT-sub7h	-43.7 ± 2.0	18.6 ± 0.2	7.5 ± 3.1	1.4	2.2	<0.5	9.6 10^{18}	0.33

- *L-band EPR phantom images*

CW EPR E540 spectrometer (Bruker, Germany) (23-mm birdcage resonator)

HPHT-sub3h (10 mg mL⁻¹)

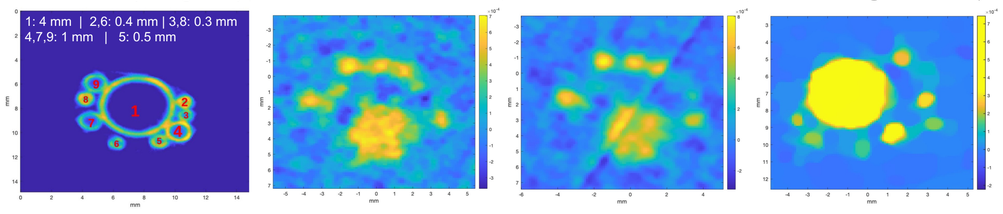

HPHT-sub3h (20 mg mL⁻¹)

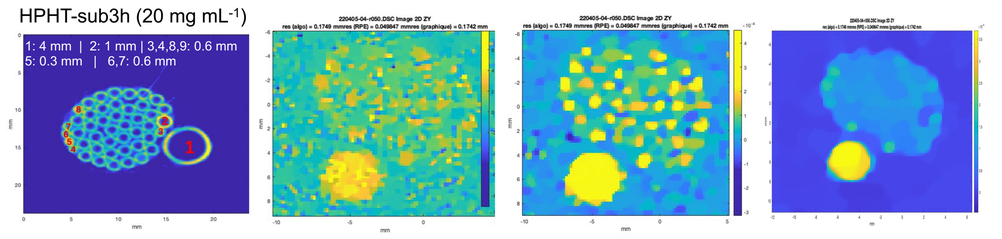

IV. Conclusions and perspectives

Summary of the presented work

- HPHT have better structural quality than DET with HPHT size approaching that of DET (5 nm size) after HPHT size exclusion
- EPR linewidth associated with surface and near-surface defects induced by grinding (dangling bonds) → decreases of the broadening EPR lines
- Functional groups (*e.g.*, carbolylic acid functions)
- HPHT-18nm and ultrasmall HPHT (<10nm) are more convenient for EPR imaging
- Stable radical-like centers
- Optimized mathematical procedures prior to imaging acquisitions

Future outlook

- Surface stabilization procedure for their use in biomedical applications

Acknowledgments: This work was performed with the financial support of the FNRS, the ARC, the Walloon Region (Protherwal and Interreg projects), the Interuniversity Attraction Poles of the Belgian Federal Science Policy Office and the COST actions. Authors thank the Center for Microscopy and Molecular Imaging (CMMI, supported by European Regional Development Fund and Wallonia). This project has received funding from European Union's Horizon 2020 research and innovation program under grant agreement No 863099.

References:
[1] S. Stehlik, *et al.*, *J Phys Chem C.* (2015) 119, 27708-20.
[2] E. Rej, *et al.*, *Nat Commun.* (2015) 6, 8459-66.
[3] Z. Peng, *et al.*, *J Chem Phys.* (2019) 13, 134702-23.
[4] DEJ. Waddington, et al., *Nat Commun.* (2017) 1, 15118-27.